^{31}P MR Spectroscopy of the Testes and Immunohistochemical Analysis of Sperm of Transgenic Boars Carried N-terminal Part of Human Mutated Huntingtin

^{31}P MR spektroskopie varlat a imunohistochemická analýza spermií transgenních kanců nesoucích N-terminální část lidského mutovaného huntingtinu

Abstract

Huntington's disease (HD) is an inherited autosomal neurodegenerative disorder characterized by motor dysfunctions, behavioral and cognitive disturbances. It affects predominantly the brain, however, changes were found also in peripheral tissues. Some of these changes can result from direct expression of mutant huntingtin; its highest levels have been found in the brain and testes. In 2009 we established a minipig model of HD (TgHD) expressing N-terminal (548aa) part of human mutated huntingtin encoded 124 CAG/CAA repeats. Previous research has revealed the presence of reduced fertility and fewer spermatozoa per ejaculate in TgHD boars started at 13 months of age. The aim of this study was to determine changes in the testes of 24 months old transgenic boars (F2 generation *in vivo*) using non-invasive methodology of ^{31}P magnetic resonance (MR) spectroscopy as well as to perform imunohistochemical analysis of TgHD sperm collected from-form F1 and F3 generation before HD onset. The results have shown significant reduction of relative phosphodiester concentration in testicular parenchyma of TgHD boars compared to wild type (WT) ones of the same ages. Moreover immunohistochemical analysis of sperm collected from TgHD and WT have revealed exclusive anti-polyQ specific (clone 3B5H10) as well as significantly increased anti-huntingtin (clone EPR5526) staining in transgenic spermatozoa tails in comparison with WT counterparts. Thus, our results are suggestive of the negative impact of human mutated huntingtin on testes metabolism as well as sperm abnormalities.

The authors declare they have no potential conflicts of interest concerning drugs, products, or services used in the study.
Autoři deklarují, že v souvislosti s předmětem studie nemají žádné komerční zájmy.
The Editorial Board declares that the manuscript met the ICMJE "uniform requirements" for biomedical papers.
Redakční rada potvrzuje, že rukopis práce splnil ICMJE kritéria pro publikace zasílané do biomedicínských časopisů.

M. Jozefovicova[1,2], V. Herynek[1], F. Jiru[1], M. Dezortova[1], J. Juhasova[3], S. Juhas[3], J. Klima[3], B. Bohuslavova[3], J. Motlik[3], M. Hajek[1]

[1] MR Unit, Department of Diagnostic and Interventional Radiology, Institute for Clinical and Experimental Medicine, Prague, Czech Republic
[2] Department of NMR Spectroscopy and Mass Spectroscopy, Faculty of Chemical and Food Technology, Slovak University of Technology, Bratislava, Slovak Republic
[3] Institute of Animal Physiology and Genetics, AS CR, v.v.i., Libechov, Czech Republic

✉
MVDr. Stefan Juhas, Ph.D.
Institute of Animal Physiology and Genetics
AS CR, v.v.i.
Rumburska 89, 277 21 Libechov
Czech Republic
e-mail: juhas@iapg.cas.cz

Accepted for review: 3. 10 2015
Accepted for print: 20. 10 2015

Key words

Huntington's disease – testes – sperm – minipig – magnetic resonance spectroscopy

Klíčová slova

Huntingtonova nemoc – varlata – spermie – miniprase – magnetická rezonanční spektroskopie

http://dx.doi.org/10.14735/amcsnn20152S28

Souhrn

Huntingtonova nemoc (HN) je autozomálně dominantně dědičné neurodegenerativní onemocnění charakterizované motorickým deficitem, poruchami chování a kognitivních funkcí. Postihuje především mozek, přičemž změny související s HN byly nalezeny rovněž i v periferních tkáních. Některé z nich mohou být způsobeny přímou expresí mutovaného huntingtinu, jehož nejvyšší koncentrace byly nalezeny v mozku a varlatech pacientů s HN. V roce 2009 jsme vytvořili miniprasečí model HN (TgHD) exprimující N-terminální (548aa) část lidského mutovaného huntingtinu kódujícího 124 CAG/CAA repetic. Na základě předchozích experimentů byla u TgHD kanců od 13. měsíce věku zjištěna zhoršená schopnost reprodukce a snížený počet spermií v ejakulátu. Cílem této studie bylo prokázat změny ve varlatech 24 měsíčních transgenních kanců (F2 generace *in vivo*) pomocí neinvazivní metody ^{31}P magnetické rezonanční spektroskopie a provést imunohistochemickou analýzu TgHD spermií odebraných z F1 a F3 generace před projevením se klinických příznaků HN. Na základě vyšetření magnetickou rezonancí bylo zjištěno signifikantní snížení relativní koncentrace fosfodiesterů v testikulárním parenchymu TgHD kanců v porovnání s netransgenními jedinci (WT) stejné věkové kategorie. Rovněž imunohistochemická analýza spermií odebraných z TgHD a WT kanců odhalila výrazné anti-polyQ specifické (klon 3B5H10) stejně tak i signifikantně zvýšené anti-huntingtin (klon EPR5526) barvení v bičících transgenních spermiích v porovnání s netransgenními spermiemi. Na základě našich výsledků lze usuzovat, že lidský mutovaný huntingtin má negativní vliv na metabolizmus varlat a způsobuje zvýšený výskyt abnormalit spermií.

Aim/s of the study

Huntington's disease (HD) is a progressive neurodegenerative disorder caused by an unstable CAG (cytosine-adenine-guanine) trinucleotide expansion in the huntingtin gene (HTT) on the short arm of chromosome 4 [1,2]. Symptoms such as motor dysfunctions, behavioral and cognitive disturbances [3] have been early linked to neurodegeneration occurring in the brain [4]. However, abnormal changes were also found in peripheral tissues like testes, heart, pancreas, skeletal muscle [5]; some of these changes can result from direct expression of mutant huntingtin [4] or a loss of wild type one [6]. The highest levels of huntingtin expression have been found in the brain and testes [4]. Indeed, the human brain and testes have the most similar gene expression pattern in compare with other organ types [7]. It has been also shown that men with HD have reduced numbers of germ cells (spermatocytes, spermatids) and abnormal seminiferous tubule morphology in the testis [8]. In addition mutant huntingtin not only compromised spermatogenesis in HD patients but also in R6/2 [9] and YAC128 [8] mouse models. Infertility in the R6/2 males was due either to death of GnRH neurons or to a reduction in GnRH expression leading to a downstream impairment of the gonadotropic hormones [9]. On the other side the testes atrophy and decline in sperm production and final azoospermia in R6/2 mice occurs at the time of onset of neuropathological symptoms and all of them were sterile by eight weeks of age [5]. In the YAC128 mouse model, testicular degeneration develops prior to 12 months of age, but at 12 months, there is no evidence for decreased testosterone levels or loss of GnRH neurons in the hypothalamus [8]. As we have reported previously, HD porcine model shows lower spermatozoa counts compared to wild type animals [10]. In addition motility and oocyte penetration capability of sperm is reduced in transgenic boars bearing mutant huntingtin [11] and indicates defects in its spermatogenesis. The mechanism of mutant huntingtin action on cell functions is not completely known as it interacts with a plethora proteins and localizes to various cellular structures like the nucleus, Golgi apparatus, mitochondria etc. [12–16]. Recently mutant huntingtin has been shown to bind to the basal body and to interfere with cilliogenesis [17–19]. Thus insight into pathogenesis occurring in the testis and spermatogenesis of men and animal models of HD may reveal common critical pathways which lead to degeneration in the brain and other organs.

^{31}P MR spectroscopy is a non-invasive method that can be used to monitor the metabolite changes of different tissue types like the brain, liver, muscle and testes *in vivo* [20–25]. The *in vivo* ^{31}P MR spectrum of the testis contains seven characteristic peaks originating from phosphomonoesters (PME), phosphodiesters (PDE), adenosine triphosphate (three peaks representing three phosphates ATP-α, -β, -γ), inorganic phosphate (Pi), and phosphocreatine (PCr), which is not present in the testicle, but arises from a muscle contamination [23]. In the spectrum can be also identified small signal of nicotinamide adenine dinucleotide (NADH). PME peak represents mainly phosphocholine and phosphoethanolamine and is directly related to the rate of phospholipid biosynthesis. The PDE peak reflects phospholipid breakdown and mostly consists of glycerophosphocholine and glycerophosphoethanolamine. Inorganic phosphate is a catabolic product of metabolites containing phosphates [25–27]. Moreover ^{31}P MR spectroscopy of the human testes may differentiate between normal testes, oligozoospermia, azoospermia that is caused by epididymal obstructions in the reproductive tract (normal spermatogenesis) and azoospermia that is caused by testicular failure (no germ cells are present) [23].

The minipig boars have huge testis, what allowed big voxel size in this area. In addition the minipig males also produce a large volume of sperm as an optimal biological material collected by noninvasive approach.

The aim of this study was to determine changes in the testes and sperm of transgenic minipigs expressing human mutated huntingtin related to testicular abnormalities by using ^{31}P MR spectroscopy and immunohistochemistry.

Methods

Minipigs

Transgenic boars (TgHD) according to [10] were obtained from The Institute of Animal Physiology and Genetics (Libechov, Czech Republic). The minipig strain resulted from Minnesota, Gottingen, and domestic farm strain cross-breeding and their successful germ line transmission occurred through successive F0, F1, F2 and F3 generations. Until now several phenotypes like the reduced male reproductive parameters (e. g. fewer spermatozoa per ejaculate), impaired mitochondrial function in spermatozoa [11], lower level of total creatine in the brain [28] and blood serum cytokine imbalance [29] have been detected. The founder sow, born July 2009, as well as the offsprings are without clinical symptoms of HD at the present time. We expect the outbreak of the clinical symptoms in the second half of their life, i.e., after the 10th year. Transgenic boars

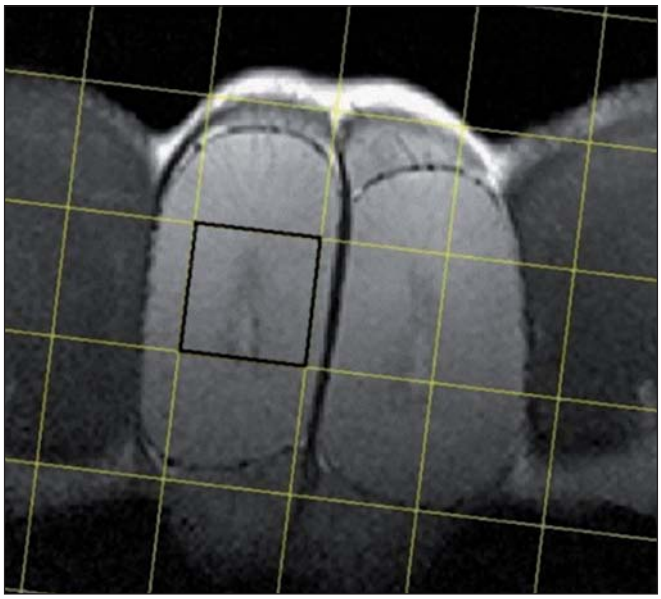

Fig. 1. The positioning of the spectroscopic grid in the program jSIPRO.

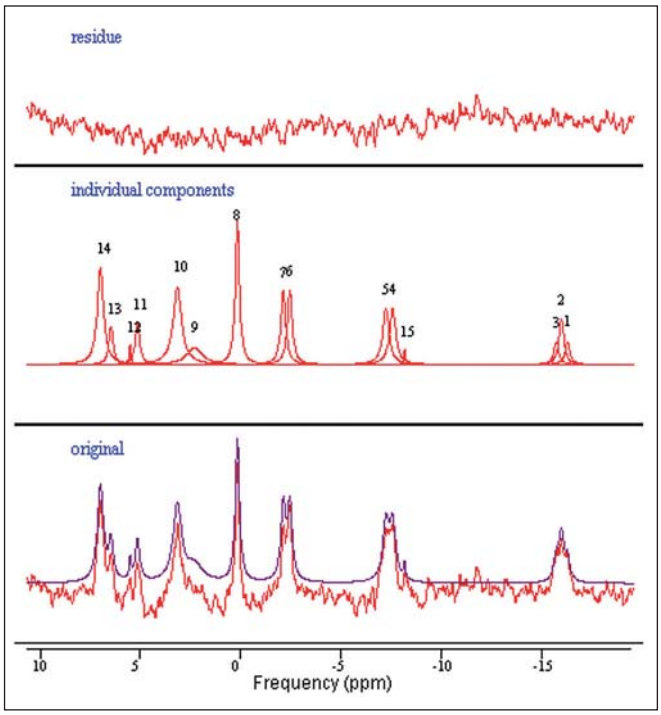

Fig. 2. Quantification of representative spectrum from one voxel in testis in the program AMARES.

Teoretical fitted spectrum (middle) obtained by a quantification of the experimental spectrum (below) is denoted with a blue color. Upper image shows residual.

from F2 generation (2 years old) before HD onset (n = 5) and control wild type (WT) siblings (n = 5) were used for MR spectrometry study. For sperm IHC study we used transgenic and WT boars from F1 (n = 2; 4–5 years old) and F3 (n = 2; 2 years old).

In MR spectrometry study minipigs were anesthetized with propofolum (Propofol 1% Fresenius) in combination with intramuscular TKX mixture (Tiletaminum 5 mg/kg, Zolazepamum 5 mg/kg, Ketaminum 5 mg/kg, Xylazine 1 mg/kg). For premedication of minipigs TKX mixture in combination with diazepamum (0.25 mg/kg, Apaurin) was used. A pulse oximeter clipped to a tail for continuous control of pulse rate and oxygen level in the blood of the minipig was used. Semen from transgenic and nontransgenic animals was collected without anesthesia using phantom dummy.

All experiments were conducted with the approval of the State Veterinary Administration of the Czech Republic and in accordance with Czech regulations and guidelines for animal welfare.

MR spectrometry experiments

All MR experiments were performed using a whole body 3T MR scanner (Siemens Magnetom Trio). A flexible dual tuned ^{1}H/^{31}P surface coil (Rapid Biomedical, Rimpar, Germany) was placed beneath the animal in a prone position. For spectra localization, three perpendicular images obtained by a standard T2W turbo-spin echo sequence (TR = 4 400 ms, TE = = 99 ms, slice thickness = 4 mm), were used. ^{31}P spectra were acquired by 2D-CSI (Two-Dimensional Chemical Shift Imaging) sequence (TR = 4 000 ms, TE = 2 ms, VOI = 240 × 240 × 25 mm, matrix size 8 × 8 × 1, voxel size 30 × 30 × 25 mm, NA = 8). The positioning of the voxel in 2D-CSI spectroscopic grid is shown in Fig. 1. An automatic magnetic field homogeneity adjustment based on B0 mapping supplemented by manual shimming was used.

MR spectrometry post-processing

Data were preprocessed using a program jSIPRO [30] which involved k-space Hamming filtering and shifting of the spectroscopic grid for the best fit positioning of the selected voxel in the area of the testis. The single spectrum from the chosen voxel was exported as a text file and then processed in the jMRUI software package (version 5.0). Processing involved manual phase correction (zero and first-order), hard phase of all signals and setting of the reference (PCr) peak to 0 ppm. Spectra were analyzed using the AMARES algorithm [31], which is a part of jMRUI software package [32]. Eight signals were evaluated in each spectrum. PCr and NADH peaks were fitted as singlets, Pi, PME, PDE as two singlet peaks (with restricted linewidths to maximal value 100 Hz), α-ATP, γ-ATP peaks as doublets, and β-ATP as a triplet. Signal of α-ATP, β-ATP and γ-ATP peaks were not constraint to each other because the integrals of α-ATP, γ-ATP signals might also contain contribution of adenosine diphosphate (ADP). For all signals a Lorentzian shape was used.

The spectra quantification was performed without fixed values of zero and first-order phase by using weighting function (quarter-sine wave) in an interval 1–10 and truncation of first 2 points of the FID.

The relative metabolite concentrations were calculated as ratios to γ-ATP. We are aware that the γ-ATP signal may also include a contribution from ADP. However, although β-ATP signal would be unambiguous, it might be affected by the partial excitation due to its large chemical shift displacement, hence it is not suitable as a reference [22,33]. The testicular spectra from minipigs were contaminated by the signals from muscle, as evidenced by the presence of PCr signal in the spectra. Therefore the ATP and Pi concentrations were corrected by deduction of the muscle contribution calculated from the PCr signal. Muscle ATP (20% of the PCr signal) and Pi (10% of the PCr signal) contribution was determined from the spectra in the

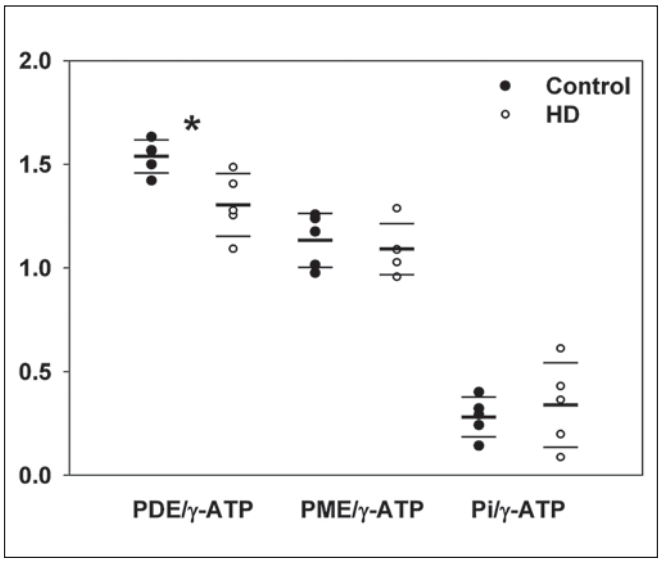

Fig. 3. Distribution of the ratios PDE/γ-ATP, PME/γ-ATP and Pi/γ--ATP in the group of TgHD minipigs (○) and control wild type (nontransgenic) siblings (•).

Horizontal lines show average values and standard deviations. Asterix marks significance level $p < 0.05$.

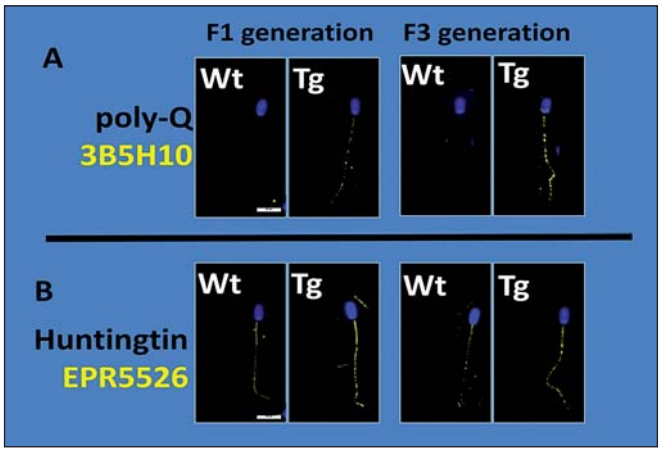

Fig. 4. Immunofluorescence staining of transgenic (Tg) and control (Wt) boar spermatozoa (F1 and F3 generation).

Fig. 4A) Using 3B5H10 antibody, no poly-Q specific signal was found in WT spermatozoa. Distinct 3B5H10 positive signal (yellow) was detected solely in transgenic HD spermatozoa.

Fig. 4B) Anti-huntingtin specific antibody EPR5526 revealed huntingtin epitopes either in WT and Tg spermatozoa of both generations. The punctuate staining was more intensive in Tg than in WT spermatozoa. Sperm heads were counterstained with DAPI (blue). Scale bar represents 10 μm.

muscle obtained during the same measurement (in two WT minipigs) and was in agreement with published data [24,34]. Concentrations of PME and PDE were not corrected as their concentrations in the muscle are negligible with respect to the experimental error.

IHC

The semen of F1 and F3 generation boars (both genotypes) was collected using the hand-glove technique. After three times washing in BTS buffer spermatozoa were diluted to 5×10^5 concentration and cytospinned onto a microscopy slide and air dried. The prepared spermatozoa were permeabilized using 0.04% Triton in PBS for 5 min. 30 min blocking step was carried out by blocking buffer consisting of permeablization buffer supplemented with 0.2% non-fat dry milk. Anti-huntingtin (1 : 400, clone EPR5526, MABN1105, Millipore) or anti-polyQ antibody (1 : 1000, clone 3B5H10, P1874, Sigma Aldrich) were applied in blocking solution for 1 hour at room temperature. Excess of antibody was removed by three times washing in washing buffer (0.05% Tween in PBS). Goat anti-mouse or anti-rabbit secondary antibodies conjugated with Alexa 555 (1 : 500, A-21422, A-21428, Invitrogen) were used for 1 hour incubation to visualize bound primary antibodies. After three times washing stained spermatozoa were mounted in DAPI containing mounting medium and evaluated under a virtual slide system VS120-FL Olympus (Olympus, Czech Republic).

Statistics

One spectrum from each testis was obtained; i.e., two spectra from each minipig (5 TgHD and 5 WT) were evaluated. The relative concentrations (γ-ATP, e.g. PDE/γ-ATP, PME/γ-ATP and Pi/γ-ATP) were tested for normal distribution (Shapiro-Wilk test) and homogeneity of variance (Levene's tests – absolute and squared deviations). These conditions were fulfilled for all these ratios and therefore were evaluated using two-tailed Student's t-test. A level $p < 0.05$ was considered as a statistically significant difference. The value of NADH was not evaluated due to its small concentration in the spectra.

For statistical analysis of EPR5526 fluorescently stained spermatozoa an unpaired t-test and Mann-Whitney nonparametric test were employed using GraphPad PRISM software (GraphPad Software, San Diego, CA, USA).

Results

MR spectrometry

The quantification of a typical spectrum from one testis using the program AMARES is shown in Fig. 2.

The ratios PDE/γ-ATP, PME/γ-ATP and Pi/γ-ATP of the WT and TgHD minipigs are displayed in Fig. 3. Distribution within the experimental groups and average values including standard deviations are also presented. We found significant decrease in the ratio PDE/γ-ATP ($p = 0.022$) in TgHD animals compared to WT and no difference in relative PME and Pi concentrations.

IHC

Ejaculated boar spermatozoa were specifically stained with anti-polyQ specific antibody clone 3B5H10. F1 and F3 generation of transgenic spermatozoa showed punctuate fluorescence signal along the whole sperm tail, whereas there was no 3B5H10 signal in tails of wild type (Fig. 4A) spermatozoa. Contrary to expectation 3B5H10 staining was missing in mitochondrion of both genotypes. EPR5526 antibody raised against N-terminal part of huntingtin protein showed similar punctuates staining in both genotypes (Fig. 4B). However, the fluorescence signal was stronger in transgenic spermatozoa and resulted into statistical significance (Fig. 5).

Conclusion

HD is a neurodegenerative disorder that besides the brain affects also peripheral organs like the testes. However it is still unclear whether these abnormal changes are result

from direct toxicity of the mutant huntingtin in the peripheral organ or they are a consequence of the brain damage [8,35].

TgHD minipig fertility problems manifested themselves in the reduced male reproductive parameters; nevertheless the minipigs were up to now without typical clinical manifestations (uncontrolled muscle movements, weight loss, etc.) of HD.

Determination of changes in the testes has been mainly based on analysis of seminal fluid or level of hormone concentrations so far [27], because biopsy is invasive and may cause additional damage to spermatogenesis [23]. ^{31}P MR spectrometry is a non-invasive technique that can be used to monitoring the testicular function as shown in several studies [23–26]. Importantly, this paper represents the first ^{31}P CSI spectroscopy of HD large animal model testes.

For the measurement of human or rats testes ^{31}P non-localized or localized single volume spectroscopy were used. Multivoxel spectroscopy might fail due to anatomical conditions of the testes [23,24,26,36]. However, anatomical size of minipig's testes allows multivoxel measurements with relatively big voxel size in this area (30 × × 30 × 25 mm), therefore we used spatially resolved multivoxel spectroscopic method Chemical Shift Imaging (CSI).

In earlier studies spectra were quantified by simple integration of individual peaks [25,26]. We used a program AMARES instead, which is commonly used for analysis of ^{31}P MR spectrometry spectra.

Previous ^{31}P MR spectrometry studies of the human testes demonstrated that the PME/ATP ratio is a more sensitive parameter to monitor testicular function, i.e., to differentiate between normal testes, oligozoospermia and azoospermia, than the PDE/ATP or Pi/ATP ratio [24,27]. However, we have not found a significant change in PME/ATP ratio in our study with HD minipigs. Nevertheless we should admit that small numbers of the animals in WT and TgHD groups was a limiting factor in this study.

It has been shown that PDE peak mainly consists of glycerophosphocholine (GPC) and in smaller amount of glycerophosphoethanolamine (GPE) [25]. GPC is present in very high concentrations in seminal fluid and a positive correlation was found between the GPC concentration and sperm motility [25,37]. Therefore we suggest that a decreased level of PDE/γ-ATP ratio in TgHD minipigs may be related to decreased concentration of seminal fluid or the changes in sperm motility. Similar reduction in the testicular phosphodiesters (PDE) PDE/ATP ratio ($p < 0.05$) as we have observed in our TgHD minipig study has been detected in rats that were pair-fed for 10 weeks on ethanol containing liquid diet (36% ethanol of total calories) [38].

The aim of sperm IHC study was to focus on the localization of huntingtin protein in spermatozoa as the sperm flagellum is a modified primary cilium and also contains mitochondria. Using poly-Q specific staining we could clearly discriminate transgenic and wild type spermatozoa respectively. Huntingtin specific staining localized endogenous porcine huntingtin as well as mutant N-terminal part of human huntingtin to the tail (flagellum) of the porcine sperm. Both staining protocols showed punctate staining along the midpiece and principal piece. This indicates huntingtin protein localization to either axonemal structures or outer dense fibers. Our data cannot support huntingtin localization to mitochondria.

Finally we studied transgenic minipigs (F1, F2 and F3 generation) expressing mutant huntingtin without clinical symptoms of HD at the time of the study. Until now several phenotypes like the reduced male reproductive parameters were detected which manifest themselves by decrease of relative PDE concentration in the testes revealed by ^{31}P MR spectroscopy. We hypothesize that the PDE decrease was related to decreased concentration of seminal fluid or the changes in sperm motility. These findings were in agreement with immunofluorescent detection of N-terminal fragment of human huntingtin in tails of spermatozoa collected from TgHD boars.

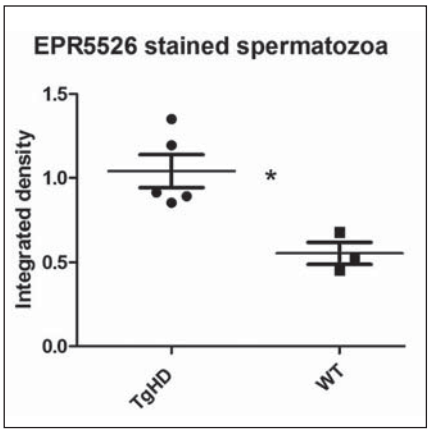

Fig. 5. Quantification of fluorescent signal in TgHD (n = 5) and WT (n = 3) boars´ spermatozoa (F1 and F3 generation).

Integrated densities of five randomly selected spermatozoa from each animal (TgHD and WT) were measured by image processing program ImageJ (Rasband, W.S., U. S. National Institutes of Health, Bethesda, Maryland, USA). Asterisk marks significance level $p < 0.05$.

Acknowledgements

This work was supported by the MH CZ-DRO („Institute for Clinical and Experimental Medicine – IKEM, IN 00023001"), Program Research and Development for Innovation Ministry of Education, Youth and Sports ExAM CZ.1.05/2.1.00/03.0124, Norwegian Financial Mechanism 2009–2014 and the Ministry of Education, Youth and Sports under Project Contract no. MSMT-28477/2014 "HUNTINGTON" 7F14308, CHDI Foundation (A-5378, A-8248) and RVO: 67985904.

References

1. van den Bogaard SJ, Dumas EM, Teeuwisse WM, Kan HE, Webb A, Roos RA et al. Exploratory 7-Tesla magnetic resonance spectroscopy in Huntington's disease provides in vivo evidence for impaired energy metabolism. J Neurol 2011; 258(12): 2230–2239. doi: 10.1007/s00415-011-6099-5.

2. van Oostrom JC, Sijens PE, Roos RA, Leenders KL. 1H magnetic resonance spectroscopy in preclinical Huntington's disease. Brain Res 2007; 1168: 67–71.

3. Bano D, Zanetti F, Mende Y, Nicotera P. Neurodegenerative processes in Huntington's disease. Cell Death Dis 2011; 2: e228. doi: 10.1038/cddis.2011.112.

4. van der Burg JM, Bjorkqvist M, Brundin P. Beyond the brain: widespread pathology in Huntington's disease. Lancet Neurol 2009; 8(8): 765–774. doi: 10.1016/S1474-4422(09)70178-4.

5. Sathasivam K, Hobbs C, Turmaine M, Mangiarini L, Mahal A, Bertaux F et al. Formation of polyglutamine inclusions in non-CNS tissue. Hum Mol Genet 1999; 8(5): 813–822.

6. Dragatsis I, Levine MS, Zeitlin S. Inactivation of Hdh in the brain and testis results in progressive neurodegeneration and sterility in mice. Nat Genet 2000; 26(3): 300–306.

7. Guo J, Zhu P, Wu C, Yu L, Zhao S, Gu X. In silico analysis indicates a similar gene expression pattern between human brain and testis. Cytogenetic Genome Res 2003; 103(1–2): 58–62.

8. Van Raamsdonk JM, Murphy Z, Selva DM, Hamidizadeh R, Pearson J, Petersen A et al. Testicular degeneration in Huntington's disease. Neurobiol Dis 2007; 26(3): 512–520.

9. Papalexi E, Persson A, Bjorkqvist M, Petersen A, Woodman B, Bates GP et al. Reduction of GnRH and infertility in the R6/2 mouse model of Huntington's disease. Eur J Neurosci 2005; 22(6): 1541–1546.

10. Baxa M, Hruska-Plochan M, Juhas S, Vodicka P, Pavlok A, Juhasova J et al. A transgenic minipig model of Huntington's disease. J Huntingtons Dis 2013; 2(1): 47–68. doi: 10.3233/JHD-130001.

11. Macakova M, Hansikova H, Antonin P, Hajkova Z, Sadkova J, Juhas S et al. Reproductive parameters and mitochondrial function in spermatozoa of F1 and F2 minipig boars transgenic for N-terminal part of the human mutated huntingtin. J Neurol Neurosurg Psychiatry 2012; 83: A16–A16.

12. del Toro D, Alberch J, Lazaro-Dieguez F, Martin-Ibanez R, Xifro X, Egea G et al. Mutant huntingtin im-

pairs post-Golgi trafficking to lysosomes by delocalizing optineurin/Rab8 complex from the Golgi apparatus. Mol Biol Cell 2009; 20(5): 1478–1492.
13. Oliveira JM, Jekabsons MB, Chen S, Lin A, Rego AC, Goncalves J et al. Mitochondrial dysfunction in Huntington's disease: the bioenergetics of isolated and in situ mitochondria from transgenic mice. J Neurochem 2007; 101(1): 241–249.
14. Enokido Y, Tamura T, Ito H, Arumughan A, Komuro A, Shiwaku H et al. Mutant huntingtin impairs Ku70-mediated DNA repair. J Cell Biol 2010; 189(3): 425–443. doi: 10.1083/jcb.200905138.
15. Jeon GS, Kim KY, Hwang YJ, Jung MK, An S, Ouchi M et al. Deregulation of BRCA1 leads to impaired spatiotemporal dynamics of gamma-H2AX and DNA damage responses in Huntington's disease. Mol Neurobiol 2012; 45(3): 550–563. doi: 10.1007/s12035-012-8274-9.
16. Chiu FL, Lin JT, Chuang CY, Chien T, Chen CM, Chen KH et al. Elucidating the role of the A2A adenosine receptor in neurodegeneration using neurons derived from Huntington's disease iPSCs. Hum Mol Genet 2015; pii: ddv318.
17. Keryer G, Pineda JR, Liot G, Kim J, Dietrich P, Benstaali C et al. Ciliogenesis is regulated by a huntingtin-HAP1-PCM1 pathway and is altered in Huntington's disease. J Clin Invest 2011; 121(11): 4372–4382. doi: 10.1172/JCI57552.
18. Kaliszewski M, Knott AB, Bossy-Wetzel E. Primary cilia and autophagic dysfunction in Huntington's disease. Cell Death Differ 2015; 22(9): 1413–1424. doi: 10.1038/cdd.2015.80.
19. Haremaki T, Deglincerti A, Brivanlou AH. Huntingtin is required for ciliogenesis and neurogenesis during early Xenopus development. Dev Biol 2015; pii: S0012-1606(15)30057-9. doi: 10.1016/j.ydbio.2015.07.013.
20. Bogner W, Chmelik M, Schmid AI, Moser E, Trattnig S, Gruber S. Assessment of (31)P relaxation times in the human calf muscle: a comparison between 3 T and 7 T in vivo. Magn Reson Med 2009; 62(3): 574–582. doi: 10.1002/mrm.22057.
21. Novak J, Wilson M, Macpherson L, Arvanitis TN, Davies NP, Peet AC. Clinical protocols for 31P MRS of the brain and their use in evaluating optic pathway gliomas in children. Eur J Radiol 2014; 83(2): e106–e112. doi: 10.1016/j.ejrad.2013.11.009.
22. Schmid AI, Chmelik M, Szendroedi J, Krssak M, Brehm A, Moser E et al. Quantitative ATP synthesis in human liver measured by localized 31P spectroscopy using the magnetization transfer experiment. NMR Biomed 2008; 21(5): 437–443.
23. van der Grond J, Laven JS, Lock MT, te Velde ER, Mali WP. 31P magnetic resonance spectroscopy for diagnosing abnormal testicular function. Fertil Steril 1991; 56(6): 1136–1142.
24. van der Grond J, Laven JS, te Velde ER, Mali WP. Abnormal testicular function: potential of P-31 MR spectroscopy in diagnosis. Radiology 1991; 179(2): 433–436.
25. van der Grond J, Laven JS, van Echteld CJ, Dijkstra G, Grootegoed JA, de Rooij DG et al. The progression of spermatogenesis in the developing rat testis followed by 31P MR spectroscopy. Magn Reson Med 1992; 23(2): 264–274.
26. Srinivas M, Degaonkar M, Chandrasekharam VV, Gupta DK, Hemal AK, Shariff A et al. Potential of MRI and 31P MRS in the evaluation of experimental testicular trauma. Urology 2002; 59(6): 969–972.
27. van der Grond J. Diagnosing testicular function using 31P magnetic resonance spectroscopy: a current review. Hum Reprod Update 1995; 1(3): 276–283.
28. Jozefovicova M, Herynek V, Jiru F, Dezortova M, Juhasova J, Juhas S et al. Minipig model of Huntington's disease: 1H magnetic resonance spectroscopy of the brain. Physiol Res 2015: in press.
29. Benova I, Skalnikova HK, Klima J, Juhas S, Motlik J. Activation of cytokine production in F1 and F2 generation of miniature pigs transgenic for N-terminal part of mutated human huntingtin. J Neurol Neurosurg Psychiatry 2012; 83: A16.
30. Jiru F, Skoch A, Wagnerova D, Dezortova M, Hajek M. jSIPRO – analysis tool for magnetic resonance spectroscopic imaging. Comput Methods Programs Biomed 2013; 112(1): 173–188. doi: 10.1016/j.cmpb.2013.06.018.
31. Vanhamme L, van den Boogaart A, Van Huffel S. Improved method for accurate and efficient quantification of MRS data with use of prior knowledge. J Magn Reson 1997; 129(1): 35–43.
32. Naressi A, Couturier C, Castang I, de Beer R, Graveron-Demilly D. Java-based graphical user interface for MRUI, a software package for quantitation of in vivo/medical magnetic resonance spectroscopy signals. Comput Biol Med 2001; 31(4): 269–286.
33. Valkovic L, Bogner W, Gajdosik M, Povazan M, Kukurova IJ, Krssak M et al. One-dimensional image-selected in vivo spectroscopy localized phosphorus saturation transfer at 7T. Magn Reson Med 2014; 72(6): 1509–1515. doi: 10.1002/mrm.25058.
34. Kemp GJ, Meyerspeer M, Moser E. Absolute quantification of phosphorus metabolite concentrations in human muscle in vivo by 31P MRS: a quantitative review. NMR Biomed 2007; 20(6): 555–565.
35. Hannan AJ, Ransome MI. Deficits in spermatogenesis but not neurogenesis are alleviated by chronic testosterone therapy in R6/1 Huntington's disease mice. J Neuroendocrinol 2012; 24(2): 341–356. doi: 10.1111/j.1365-2826.2011.02238.x.
36. van der Grond J, Van Pelt AM, van Echteld CJ, Dijkstra G, Grootegoed JA, de Rooij DG, et al. Characterization of the testicular cell types present in the rat by in vivo 31P magnetic resonance spectroscopy. Biol Reprod 1991;45(1):122–127.
37. Hinton BT, Setchell BP. Concentrations of glycerophosphocholine, phosphocholine and free inorganic phosphate in the luminal fluid of the rat testis and epididymis. J Reprod Fertil 1980; 58(2): 401–406.
38. Farghali H, Williams DS, Gavaler J, Van Thiel DH. Effect of short-term ethanol feeding on rat testes as assessed by 31P NMR spectroscopy, 1H NMR imaging, and biochemical methods. Alcohol Clin Exp Res 1991; 15(6): 1018–1023.